Current Biology, Vol. 14, 1330–1340, August 10, 2004, ©2004 Elsevier Ltd. All rights reserved. DOI 10.1016/j.cub.2004.07.028

Laser Microsurgery in Fission Yeast: Role of the Mitotic Spindle Midzone in Anaphase B

Alexey Khodjakov,[1,4,*] Sabrina La Terra,[1,2] and Fred Chang[3,4,*]

[1]New York State Department of Health
Wadsworth Center
P.O. Box 509
Albany, New York 12201

[2]Department of Biomedical Sciences
State University of New York, Albany
Wadsworth Center C236
Empire State Plaza
P.O. Box 509
Albany, New York 12222

[3]Department of Microbiology
Columbia University College of Physicians and Surgeons
701 W. 168th St.
New York, New York 10032

[4]Marine Biological Laboratory
Woods Hole, Massachusetts 02543

Summary

Introduction: During anaphase B in mitosis, polymerization and sliding of overlapping spindle microtubules (MTs) contribute to the outward movement the spindle pole bodies (SPBs). To probe the mechanism of spindle elongation, we combine fluorescence microscopy, photobleaching, and laser microsurgery in the fission yeast *Schizosaccharomyces pombe*.

Results: We demonstrate that a green laser cuts intracellular structures in yeast cells with high spatial specificity. By using laser microsurgery, we cut mitotic spindles labeled with GFP-tubulin at various stages of anaphase B. Although cutting generally caused early anaphase spindles to disassemble, midanaphase spindle fragments continued to elongate. In particular, when the spindle was cut near a SPB, the larger spindle fragment continued to elongate in the direction of the cut. Photobleach marks showed that sliding of overlapping midzone MTs was responsible for the elongation of the spindle fragment. Spindle midzone fragments not connected to either of the two spindle poles also elongated. Equatorial microtubule organizing center (eMTOC) activity was not affected in cells with one detached pole but was delayed or absent in cells with two detached poles.

Conclusions: These studies reveal that the spindle midzone is necessary and sufficient for the stabilization of MT ends and for spindle elongation. By contrast, SPBs are not required for elongation, but they contribute to the attachment of the nuclear envelope and chromosomes to the spindle, and to cell cycle progression. Laser microsurgery provides a means by which to dissect the mechanics of the spindle in yeast.

*Correspondence: fc99@columbia.edu (F.C.); khodj@wadsworth.org (A.K.)

Introduction

In cell biology, there is a rich history of experimentation using physical manipulation of cells. These studies have revealed the distribution of forces and overall mechanics of intracellular machinery and have contributed heavily toward our understanding of such processes as mitotic spindle formation and cytokinesis [1–3]. In recent years, laser microsurgery coupled with use of GFP-based protein markers has been developed as a powerful tool for the specific ablation of cellular structures such as the centrosome. A green laser beam, which is focused by the microscope objective, can selectively ablate intracellular structures with a spatial resolution approaching the resolution of light microscopy ($<$0.4 μm in the XY plane and 0.6 μm in the Z plane) with minimal damage to the rest of the cell [4]. This approach has been used successfully in vertebrate cells to study chromosome positioning, the functions of the centrosome, and other aspects of cell physiology [5].

While yeast cells have been invaluable experimental organisms due to their ease of genetic manipulation and dissection of molecular mechanisms, their small size and rigid cell wall prohibit the use of conventional micromanipulation techniques. Genetic approaches unveil the functions of specific proteins; however, they generally cannot be used to inactivate cellular structures at specific locations. Further, many gene products can perform multiple functions at different cell cycle stages. Although conditional alleles have allowed some degree of temporal specificity, rarely do these provide temporal resolution on the order of seconds or ensure that the cellular process assayed is entirely inactivated. New methodologies that complement the power of genetics are needed to take full advantage of the yeast model system.

Fission yeast cells undergo a closed mitosis that can be divided into four morphologically distinct phases: (1) spindle formation; (2) metaphase/anaphase A, in which spindle length remains constant at 2.5 μm for approximately 5 min; (3) anaphase B, in which the spindle elongates at approximately 1 μm/min; and (4) spindle breakdown accompanied by microtubule (MT) depolymerization when the SPBs reach the ends of the cells [6–9]. Chromosome segregation is accomplished largely by the movement of the spindle pole bodies (SPBs) in anaphase B. Electron microscopy [10] shows that fission yeast anaphase spindles contain about 25 MTs at the onset of anaphase. This number reduces to about 10 MTs in late anaphase. In the spindle, overlapping MTs from opposite SPBs form square-packed arrays with a regular spacing of 40 nm [10]. While the MT overlap zones are minimal in early anaphase, these zones increase so that by midanaphase, many MTs are bundled along at least half of their length. In late anaphase, MTs cease polymerizing and overlap only in a short segment at the spindle midzone. Both MT sliding from motor proteins such as the kinesin Cut7p (Bim1/Eg5 protein family) [11, 12] and MT polymerization at MT plus ends

are thought to contribute to spindle elongation. It is generally assumed that the MT minus ends are capped and stabilized by SPBs, but the direct experimental evidence is lacking.

Here, we have developed a combinatorial GFP-fluorescence microscopy/photobleaching/laser microsurgery approach to study the mechanics and dynamics of the mitotic spindle in yeast cells. Our results show that cuts across the spindle have different effects during different stages of anaphase. During early and late stages of anaphase, cutting through the spindle induces rapid depolymerization of MTs within the spindle. However, in midanaphase, the spindle midzone develops properties that stabilize MTs against depolymerization, and spindle fragments continue to elongate even when they are not connected to SPBs. These studies provide new insights into the regulation of MT stability and the mechanics of spindle elongation and demonstrate the utility of laser microsurgery as a new tool in the study of yeast cell biology.

Results

Laser Ablation in Fission Yeast

Although the use of laser microsurgery has been well established for experiments with mammalian tissue culture cells [4, 13], its utility in yeast cells has not been explored. Potential problems included dispersion of the laser beam by the cell wall, cell lysis, and other global cellular effects. Thus, our first goal was to demonstrate that the effects of 532 nm laser irradiation on yeast cells are identical to the effects observed by us and others in other cell types. We used the same laser beam parameters that have previously been established for the ablation of organelles in our work in mammalian cells [14–16].

Series of up to 10–20 5 ns pulses (1–2 s at 10 Hz) generally did not affect general cell integrity. Differential interference contrast (DIC) microscopy showed that yeast cells remained intact and viable, as assessed by continuous movement of intracellular components and organelles (Figure 1).

In mammalian cells, the laser pulses instantly convert all intracellular components within the focal point into amorphous electron-opaque material. The dimensions of the ablation zone are approximately 300–400 nm in the XY plane and 500–600 nm in the Z axis, as measured by same-cell electron microscopy [4]. Because of changes in refractive index, the ablated zone is easily detected in living cells by DIC microscopy [4]. We found that a series of three to five laser pulses reproducibly induced the formation of a similar small "scar" in yeast cells (Figure 1A′, insert).

To further characterize the effects of laser irradiation in yeast cells, we tested the effects of firing laser pulses through the nuclear envelope. We used cells expressing two GFP fusions: a diffusible nuclear localization signal-GFP-βgal fusion protein (NLS-GFP-βgal) that accumulates inside of the nucleus and a nuclear pore-GFP (nsp1-GFP) that marks the nuclear envelope proper [17, 18]. The rationale here was that focused laser ablation should create a hole in the nuclear envelope, leading to discharge of NLS-GFP-βgal from the nucleus. We

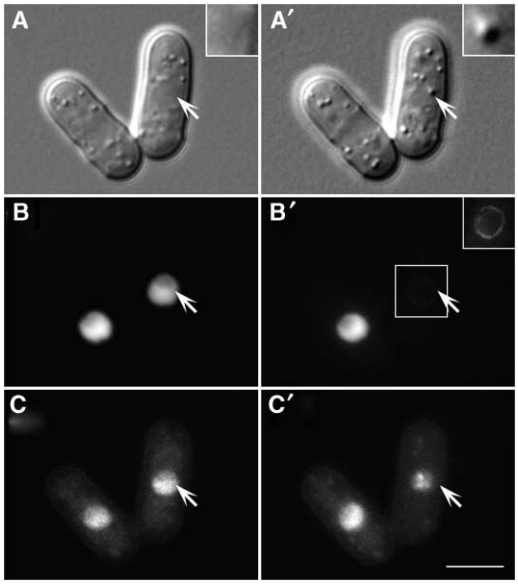

Figure 1. Laser Microsurgery Causes Specific Ablation of Cellular Structures in Fission Yeast

S. pombe cells expressing a nsp1-GFP nuclear envelope marker and a soluble NLS-GFP-βgal marker were stained with Hoechst 33342 and imaged before (A–C) and after (A′–C′) exposure to green laser pulses focused onto a region of the medial nucleus of the lower cell at the site marked by the arrow.

(A) Differential contrast interference (DIC) images. Insert shows a magnified view of a small scar formed at the cut site.

(B) GFP fluorescence images of NLS-GFP-βgal and nsp1-GFP. Insert shows an image of the same cut nucleus scaled at higher sensitivity to show the dim nsp1-GFP fluorescence at nuclear pores.

(C) Hoechst 33342 staining, showing DNA distribution. Scale bar = 5 μm.

observed that three to five laser pulses aimed at the periphery of the nucleus induced rapid loss of NLS-GFP signal (Figure 1B). Nuclear pore and chromosomal staining showed that nuclear structure remained largely intact, suggesting that the laser produced only a discrete hole in the nuclear envelope and did not, for instance, ablate the whole nucleus (Figures 1B′, insert, and 1C). Further, laser cuts in the cytoplasm adjacent to the nucleus (within 1 μm) had no detectable effects on nuclear fluorescence (our unpublished data). In cells with two nuclei (during cytokinesis), a laser cut to one of the nuclei did not affect the other (our unpublished data). These experiments established that focused 532 nm laser pulses create discrete openings in the nuclear envelope but do not compromise its integrity outside of the irradiated area. We have used a similar approach to punch holes in the membranes of mitochondria [19]. Thus the effects of laser irradiation in yeast cells were similar to those observed previously in mammalian cells [4, 14, 19].

Behavior of Uncut Mitotic Spindles

Before describing our use of laser microsurgery to cut spindles, we first present the characterization of normal spindle behavior under our particular experimental conditions. Mitotic spindles were visualized by time-lapse fluorescence microscopy in cells expressing GFP-atb2p

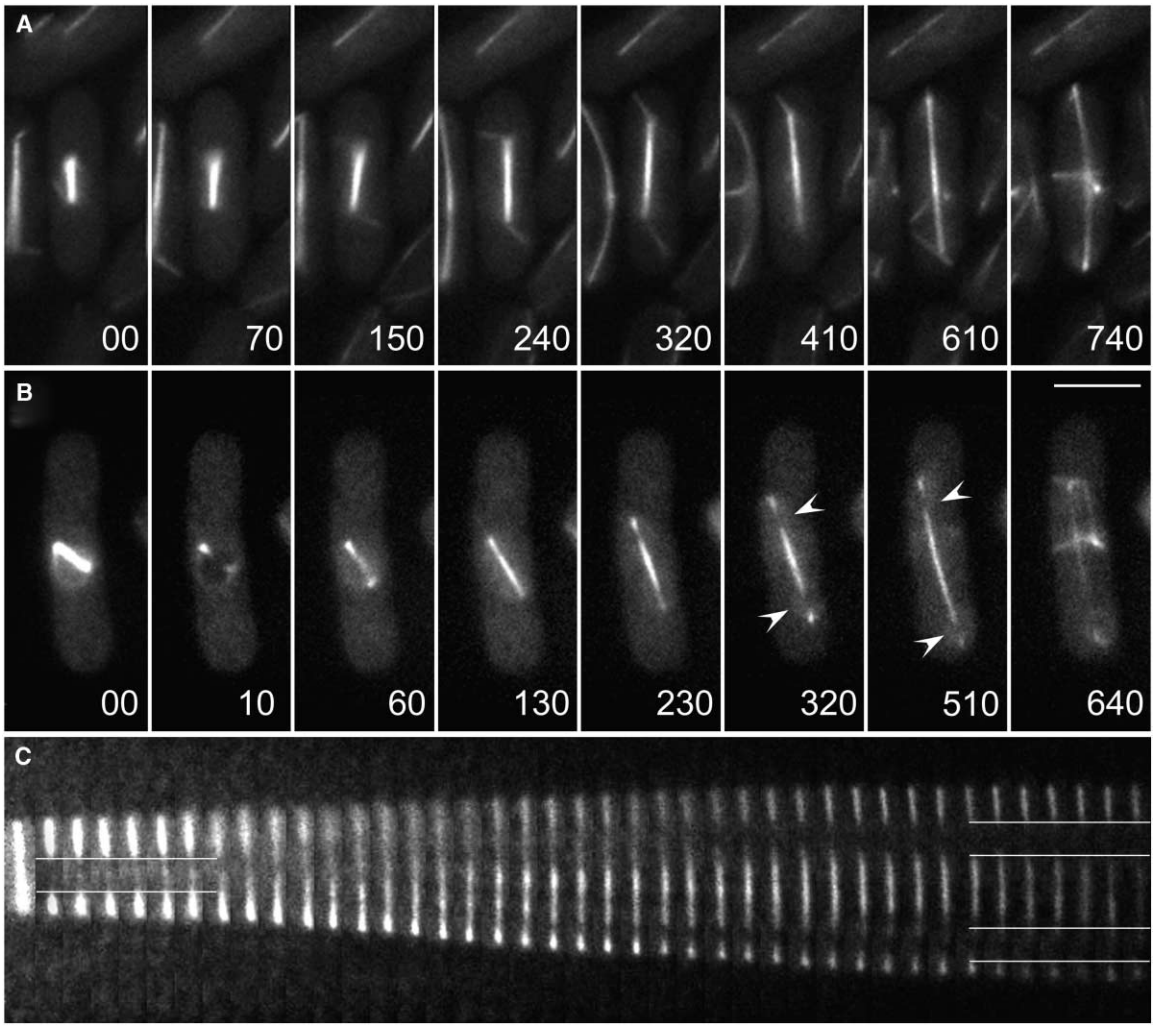

Figure 2. Stability of Microtubules in Uncut Spindles

S. pombe cells expressing GFP-α-tubulin (GFP-atb2p) were imaged by time-lapse fluorescence microscopy.

(A) Normal spindle elongation.

(B) Cell photo bleached with a low power 488 nm laser in the middle of the spindle at time 0 (arrows). Arrowheads at 320 and 510 s point to photobleach marks on the spindle that reappear later during anaphase.

(C) Kymograph showing behavior of another photo-bleached spindle over time. Each frame represents 10 s. Brackets show positions of photobleached segments. Scale bar = 5 μm.

(α-tubulin) grown on agarose pads at 28°C (Figure 2A). Consistent with previous studies [6–8], we observed that mitotic spindles in anaphase B (phase III) steadily elongated at rates of 1.1 ± 0.2 μm/min (n = 9). Postanaphase MT arrays, which are nucleated from the medial eMTOC, formed near the end of anaphase [9].

To examine the dynamics of spindle MTs, we photobleached regions of the GFP-tubulin-labeled spindle with a low power, continuous-wave 488 nm laser (see Experimental Procedures). The energy generated by this laser is not sufficient to ablate intracellular structures. We have used the same laser for photobleaching of γ-tubulin-GFP signal in mammalian cells [20], and a similar instrument was used for photobleaching mitotic spindles in yeast [21].

When we photobleached preanaphase and anaphase (2–5 μm long) spindles, GFP-tubulin fluorescence rapidly recovered in the bleached zone (Figures 2B and 2C). However, as spindles elongated, they consistently developed two dim marks near the SPBs. Importantly, the distances from the poles to adjacent bleached zones were preserved as the marks and poles moved apart (Figures 2B and 2C arrows). This behavior indicates that most, if not all, of the spindle MTs present in late spindles were also present prior to anaphase; thus, these MTs remained stable through the course of mitosis. Further, the conservation of the distance between the marks and the SPBs showed that the spindle MTs do not undergo poleward flux. The initial filling-in of the photobleach marks revealed plus-end polymerization of microtubules during anaphase. Our results are consistent with previous observations on fission and budding yeast spindles [8, 21, 22].

Laser Cuts Induce Either Depolymerization or Elongation of Spindle Fragments

To probe the properties of mitotic spindles, we used laser microsurgery to sever spindle MTs. The cuts were

Table 1. Summary of Results of Cutting Mitotic Spindles by Laser Microsurgery

	Cut Location	Result	(n)
Short spindle (2.9–4.1 μm)	Middle	Collapse	4
		Unilateral elongation	2
	Near pole	Collapse	4
		Unilateral elongation	3
Medium spindle (4.2–5.5 μm)	Middle	X-formation	5
		Collapse	1
	Near pole	Unilateral elongation	12
		Collapse	1
	Both poles	Elongation	16
		Collapse	1
Long spindle (>7.5 μm)	Middle	Collapse (to nuclear segments)	4
		Recovery	1
		No collapse, little movement	3
	Near pole	Unilateral elongation	2

Total number of cells analyzed: 59

done during various stages of anaphase B and at various points within the length of the spindle. These experiments were conducted in cells expressing GFP-α-tubulin [23, 24], and the behavior of spindle MTs was followed by time-lapse fluorescence microscopy. The results of 59 operations are summarized in Table 1.

When short and medium-length spindles were cut in the middle, an immediate response was the rapid movement of the spindle poles toward one another (Figure 3). The character of the movement did not differ between short and medium-length spindles. Importantly, astral MTs in the medium-length spindles did not appear to produce any forces that pull the spindle apart. This reveals that the forces produced within the spindle that push the poles apart is the primary force for anaphase B.

Many short spindles completely collapsed upon cutting (61%, n = 13; Figure 3A; Table 1). In these cases, all of the MTs in the nucleus progressively depolymerized so that after 100–200 s, the nucleus had no detectable MTs and was filled with depolymerized tubulin (Figure 3A). No subsequent nucleation of new MTs was detected for at least 800 s. However, laser cuts did not lead to MT depolymerization in other mitotic stages (see below), showing that the cuts were not generating global conditions (such as, perhaps, a rise in intranuclear Ca^{2+}) that would induce nonspecific MT depolymerization. The collapse was seen in both cuts to the middle of the spindle and in cuts near a pole. Thus, although MTs in uncut short spindles are stable (see above), spindle MTs are often no longer stabilized after cutting, suggesting that the cuts generate fresh MT ends that are not stabilized.

Cuts to medium-length spindles and to a subset (38%) of short spindles produced one or two spindle fragments that were stable and that continued to elongate (Table 1). When medium-length spindles were severed in the middle, both spindle halves then grew, forming an "X" pattern. In several cases, the halves of the cut spindle would "zip" together so that spindle appeared to "repair" itself and then elongated in a bilateral fashion (Figure 3D). However, time-lapse images showed that elongation was led not by the SPBs but by the part of the spindle that was previously cut. The SPBs, which often continued to nucleate astral microtubules, remained near the middle of the cell (Figure 3D, arrowhead). Thus, this abnormal structure was composed of two half spindles, each of which elongated in a unidirectional manner.

Severing of spindles off-center, near one of the SPBs, gave rise to unidirectional elongation of the larger spindle fragment (Figure 4; Table 1). While the smaller spindle fragment depolymerized rapidly, the larger spindle fragment, connected to the distal SPB, elongated in a unidirectional manner in the direction of the cut toward the cell tip. These MT "projections" elongated at an average rate of 1.2 ± 0.2 μm/min (n = 5), the same as the spindle elongation rate (1.1 μm/min) of uncut mitotic spindles grown under the same conditions. Generally, the intact pole did not move relative to the cell until the spindle projection reached the cell tip. Then, it moved away from the contact point, presumably because the continued elongation pushed the entire spindle away. The formation of the elongating MT projection was highly reproducible, especially in cuts to medium-length spindles (in 92% of asymmetric cuts to midlength spindles, n = 13, Table 1).

The fact that the final size of some MTs projections was more than 200% of the initial length of the spindle fragment implied that the elongation process could not be based solely on antiparallel MT sliding but, rather, required MT polymerization. We considered two models for how these MT projections are formed. First, the elongation of the spindle fragment may represent continued MT plus-end polymerization of MTs that originate from the distal SPB. In other words, projections may represent elongation of the distal half-spindle, where the MT plus ends grow toward the cell tip. Second, projections may represent elongation of "normal" overlapping spindle MTs. In this scenario, elongating spindle fragments may still retain overlapping MTs and may behave much like the intact spindle, except that this spindle is connected to only one SPB.

To differentiate between these two possibilities we combined laser microsurgery and photobleaching in the same cell. In these experiments, we first severed a medium-sized spindle near one of the SPB, and after the larger spindle fragment began to elongate, we photobleached it near the middle of the spindle fragment, creating a fiduciary mark (Figures 4C and 4D). Time-lapse fluorescence microscopy revealed that photobleach marks behaved in the projection just as in intact

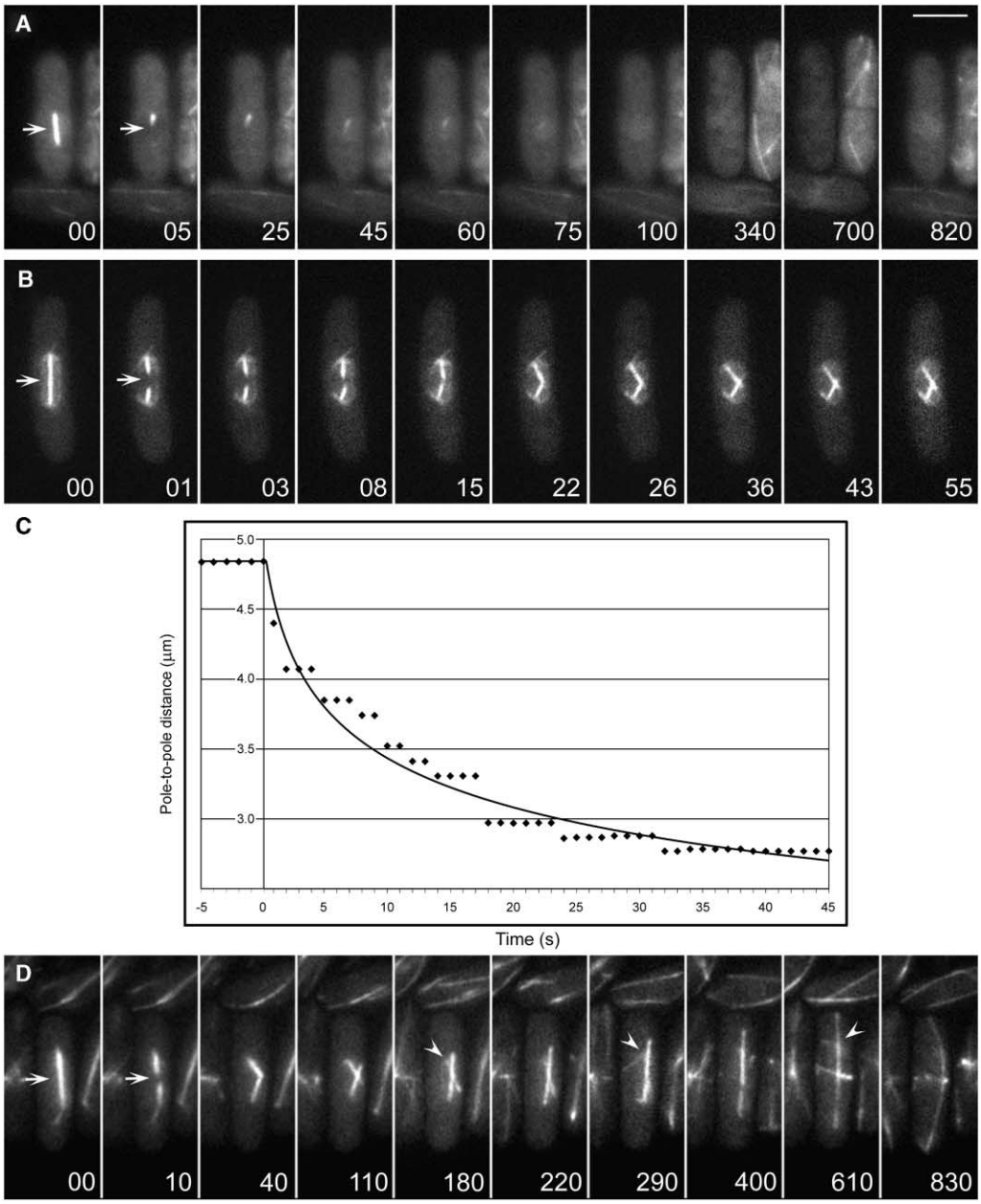

Figure 3. Behavior of Mitotic Spindles after Laser Cut: Short and Medium-Length Spindles

S. pombe cells expressing GFP-α-tubulin were imaged by time-lapse fluorescence microscopy before and after laser cut to the spindle (arrows) at time 0. Time (s) elapsed is listed.

(A) Example of a short spindle collapsing after laser cut.

(B) A medium length spindle was cut in the middle, producing an X pattern.

(C) Measurement of pole-pole distance over time of the cut spindle in (B).

(D) Another medium-length spindle cut in the middle. In this cell, spindle fragments fused and elongated. Arrowhead shows that the spindle pole body (SPB) is located on the side of the spindle, suggesting that cut end of the spindle leads the elongation. Scale bar = 5 μm.

spindles: the mark first disappeared and then reappeared as two marks at either end of the projection (n = 5 cells). As for uncut spindles, the distances from the mark to the end of the spindle were conserved. These results are inconsistent with the elongation of just one half-spindle and strongly support the second model, in which the projection contains overlapping MTs that polymerize and slide apart much like an intact spindle (Figure 4E). As the projection lacks a SPB at one of its ends, these findings show that spindles are capable of elongation in the absence of a spindle pole.

Although medium-length spindle fragments elongated similarly to intact spindles, chromosome segregation was severely compromised under these conditions. This was not surprising, considering that the site of laser ablation also contained kinetochore MTs and chromo-

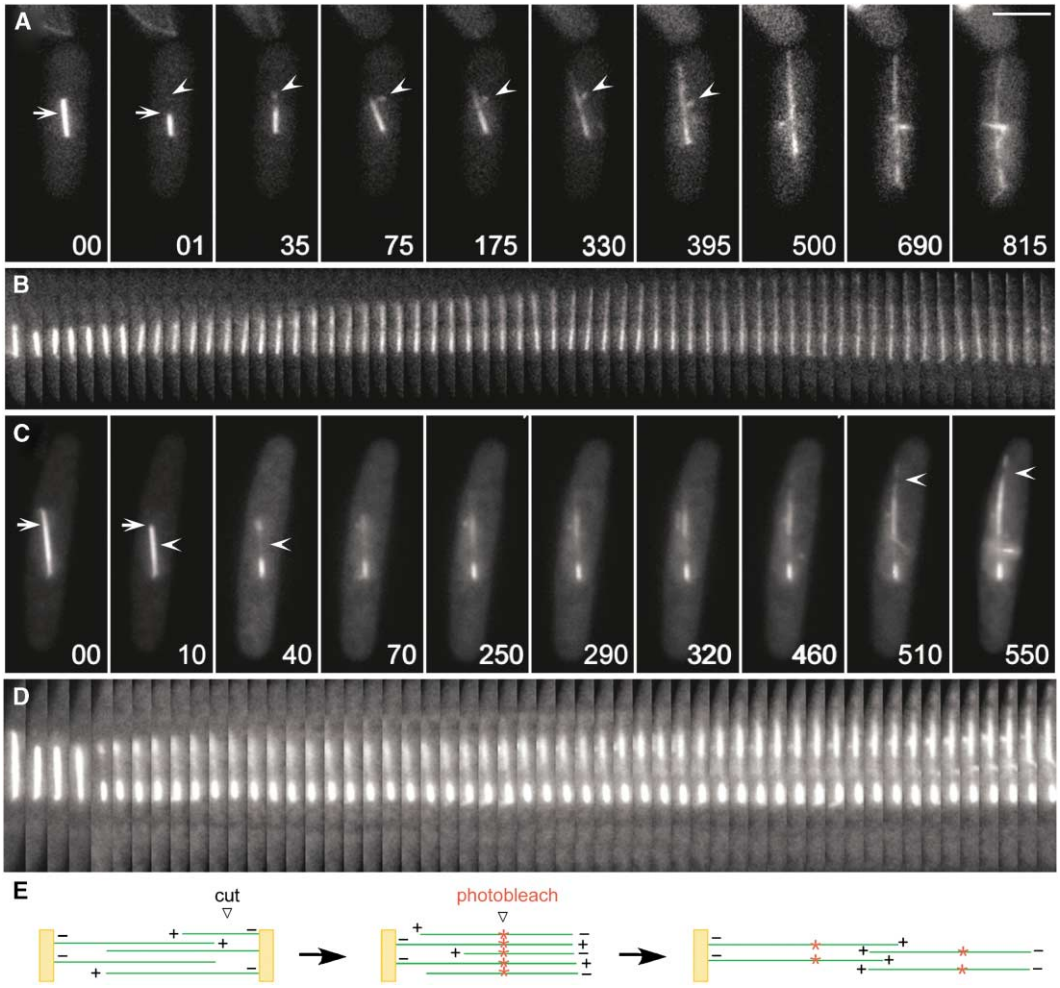

Figure 4. Elongation of a Spindle Fragment after Detachment of One Spindle Pole Body

Time lapse fluorescence images of GFP-labeled spindles that were cut asymmetrically (arrows), as to detach one of the spindle pole bodies.
(A) Example of cell that develops a unilateral projection. Note that the detached SPB (arrowhead) is associated with the side of the spindle.
(B) Kymograph of another cell. Each frame represents 10 s.
(C) Spindle was cut (arrow) and then photo bleached (arrow). The photo-bleach marks reappear near the tips of the elongated unilateral projection (arrowhead).
(D) Kymograph of the spindle shown in (C).
(E) Model of mechanism of unilateral elongation of a spindle after detachment of one SPB. Orange boxes represent SPBs. Fiduciary marks formed by photobleaching are shown in red. Plus and minus symbols represent predicted MT plus and minus ends.

somes associated with the one SPB. DNA visualization with Hoechst 33342 staining revealed that in most cases the chromosomes did not segregate equally with the elongating MT projection (Figure 5A). These asymmetric Hoechst staining patterns were not due to photobleaching by the laser (our unpublished data). Small masses of DNA were sometimes associated with the detached SPB fragment that associated with the side of the MT spindle projection. By using a nuclear pore marker (nsp1-GFP), we found that laser cuts near a SPB caused a protrusion in the nuclear envelope that grew out from the nucleus near the cut site ($n = 5$; Figures 5B and 5C). While some protrusions contained little or no nuclear contents (Figure 5C), others appeared to contain some DNA at the tip (Figure 5B). The protrusions in the nuclear envelope were presumably caused by the abnormal MT projections, as control cuts to the nuclear envelope at sites away from the SPB did not cause such effects. Thus, while MTs themselves may be able to displace the nuclear envelope, the SPBs and associated chromosomes are normally required for moving the bulk of the nuclear envelope during anaphase.

Elongation of the Spindle Midzone after Detachment of both SPBs

The results of single laser cuts to the spindles suggested that the SPB is not required for spindle stabilization or elongation. To test this idea further, we severed both SPBs from the spindle. Two cuts were made in succession on medium-length spindles, one near each SPB (Figure 6A, arrows). Remarkably, in most cases (94%, $n = 16$), the resulting spindle midzone fragment did not depolymerize but, instead, elongated. Elongation generally occurred in both directions. The fluorescence

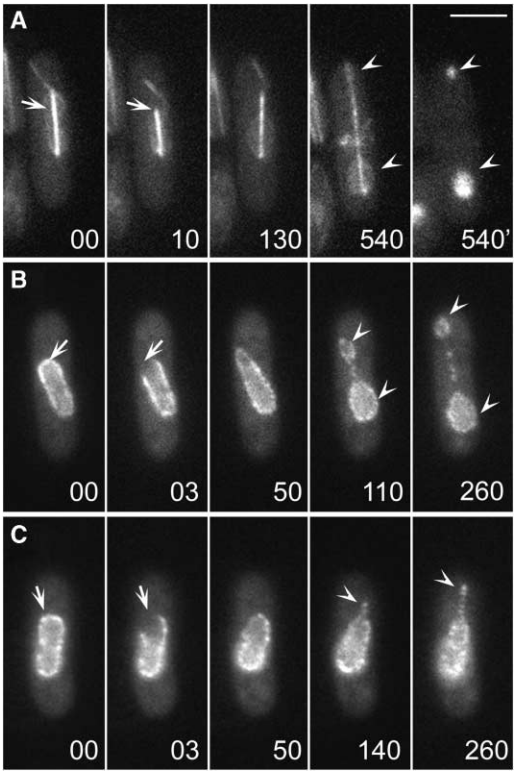

Figure 5. Effects on Chromosome Segregation and Nuclear Morphology after Laser Cuts

(A) Cell expressing GFP-α-tubulin, nup107-GFP, and stained with Hoechst 4322 was cut near one SPB (arrow). Hoechst channel (540′) shows an unequal distribution of chromosomes (arrowheads).

(B and C) Cells expressing nuclear envelope marker nsp1-GFP were cut near one SPB (arrow). Arrowheads show abnormal projections of nuclear envelope growing out from the nucleus. Scale bar = 5 μm.

intensity of these fragments was lower than that of intact spindles, suggesting that a subset of MTs was missing from these fragments. The elongation rate of these fragments was about 40% of wild-type spindle elongation rates (0.4 ± 0.1 μm/min; n = 3). Thus, the spindle can still elongate in the absence of attached SPBs.

Selective Stabilization of Microtubules in the Spindle Midzone Disappears during Telophase

Cuts in late spindles (≥7.5 μm long) caused a third behavior. Cutting the middle of these spindles caused the nuclei to abruptly move together (Figure 7), showing that as for the shorter spindles, the late spindle exerts outward-directed forces. In some cells, the spindle MTs depolymerized from the cut back to the region of the nuclei (Figure 7; Table 1). The remaining MTs then either depolymerized completely or were stabilized in the nuclear bodies. The nuclei did not collapse back into a single nucleus, possibly because by this stage, the nuclear envelope may be sealed between the daughter nuclei. In other cases, the spindle MTs did not depolymerize but were stable and did not exhibit further elongation.

Mitotic Checkpoints

The temporal specificity of laser microsurgery allows us to perturb cellular processes at very defined points in the cell cycle. In this study, we cut anaphase B spindles that were already past the spindle assembly checkpoint at metaphase [25]. In budding yeast, chromosome breakage associated with a dicentric chromosome triggers a checkpoint in mid-anaphase that delays cells with a medium-length spindle [26]. However, our observations showed that fission yeast cells with severe chromosome segregation defects (and probable chromosomal breakage) induced by laser cutting during early anaphase did not inhibit spindle elongation, suggesting that fission yeast cells do not have such a midanaphase checkpoint.

The septation initiation network (SIN) pathway functions near the end of anaphase to trigger ring closure and septation in cytokinesis and the formation of the eMTOC, which nucleates MTs from the cell division site [27, 28]. Components of the SIN pathway are thought to be localized and "active" on one of the SPBs [29].

We observed that single laser cuts near one SPB did not affect the timing of MT formation from the eMTOC (Figure 4). However, cutting off both spindle pole bodies did often cause significant delays in eMTOC activity and septation (Figure 6). Some cells never formed an eMTOC or septum in the course of the experiment (>3000 s), while others exhibited considerable delays. Although in some of these cells, the detached SPBs still nucleated MTs (usually off the side of the spindle), in other cells, the integrity of the SPBs was less clear. We tested the possible caveats that multiple laser cuts may damage the contractile ring or other cellular structures. Cuts to both SPBs did not appear to affect contractile ring integrity, as assessed by an rlc1-GFP (regulatory myosin light chain) fusion (data not shown). Other cells that received multiple cuts, in which one of the laser cuts did not completely sever the SPB, showed no delay in eMTOC formation (data not shown). Although these findings are suggestive of effects on the function of the SIN pathway, further examination of SIN pathway components will be needed to address more directly the effects on these proteins.

Discussion

The knowledge of MT dynamics and MT-based force production in the mitotic spindle is essential for understanding the mechanism of mitosis. Here, we have used the combination of laser microsurgery and photobleaching to gain new insights into the mechanism of anaphase B in fission yeast. In particular, these studies show that the spindle midzone, in the absence of SPBs, is sufficient for MT stabilization and for production of the pushing forces that drive spindle elongation.

Microtubule Stabilization

Although mitotic spindles are generally thought to be dynamic structures, *S. pombe* spindles contain a population of very stable MTs. Photobleach marks reveal that the same MTs present in the developing mitotic spindle in prophase end up as the primary MTs in the spindle at the end of mitosis (Figure 2) [8, 21]. After collapse of a cut anaphase B spindle, no new nucleation of MTs is apparent, suggesting that the MT nucleation activity in SPBs is turned off by this stage. Thus, in contrast to

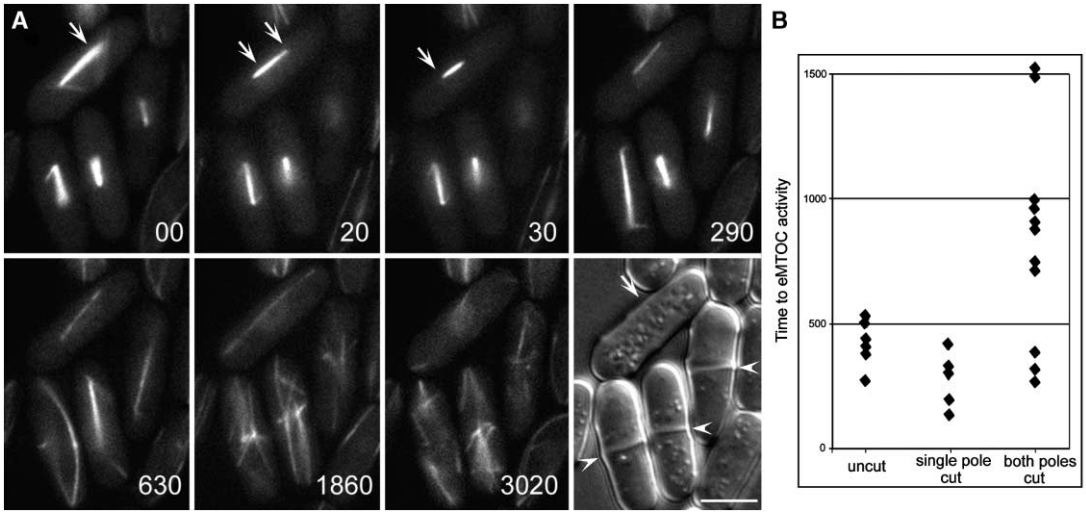

Figure 6. Elongation of a Spindle Fragment and Delay in eMTOC Formation after Detachment of Both Spindle Pole Bodies

(A) Time-lapse fluorescence and DIC (last panel) images of GFP-α-tubulin-expressing cells. The spindle of the top cell was cut twice near each SPB (from 0–30 s; arrows). The resulting spindle midzone fragment elongated (time frames 30 s to 3020 s). The cell did not form equatorial MTs or a septum (arrow in DIC image). Bottom three uncut cells exhibit elongating spindles, formation of equatorial MTs, and septum formation (arrowheads in DIC image).

(B) Measurements of the time period to eMTOC activation, as seen by the first detectable formation of equatorial MTs. In uncut cells, the time was measured from when the anaphase spindle length was 4 μm. In cut cells, all the times were derived from spindles that were 4–6 μm in length at time 0 at cutting. The top point represents cell in (A) that did not activate the eMTOC for >3000 s. Scale bar = 5 μm.

the behavior of mitotic spindle MTs in higher eukaryotes, most spindle MTs in *S. pombe* are likely to be nucleated within a short period during prophase so that spindle elongation in anaphase B occurs through the growth and movement of preexisting MTs.

Our results show that MTs are extensively stabilized within the spindle. Normally, MT minus ends, which are embedded in the SPBS, are stable; therefore most, if not all, *S. pombe* spindle MTs do not undergo the poleward flux that is characteristic of most mitotic spindles in higher eukaryotes (Figure 2) [8, 21, 30, 31]. Our laser cuts further demonstrate that midanaphase spindles must contain activities that stabilize both MT plus and minus ends at spindle cut sites, distinct from the SPBs. Photobleaching results show that overlapping antiparallel MTs are maintained in the spindle fragment after laser cut (Figure 4), indicating that the fresh MT minus and plus ends at the cut sites must be stabilized from depolymerization. In addition, the subsequent elongation of these fragments indicates that the MT plus ends must

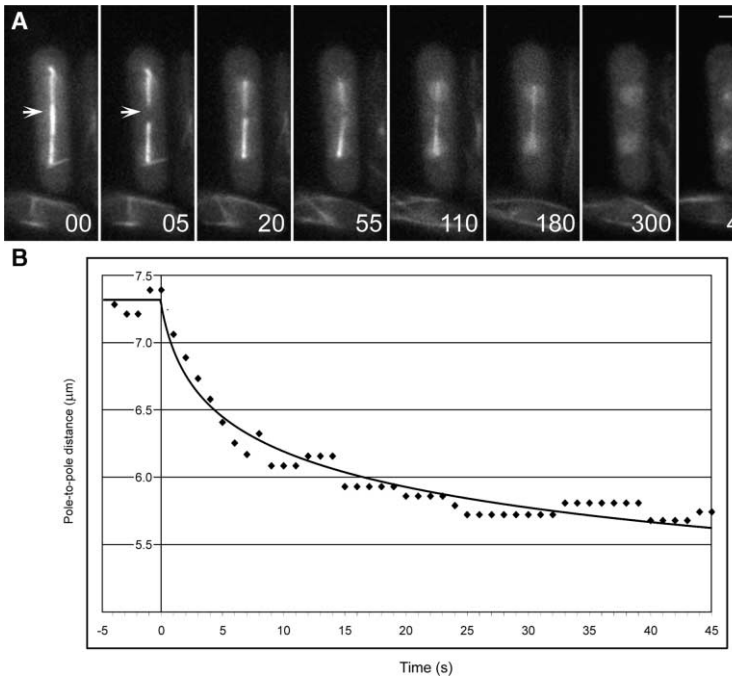

Figure 7. Collapse of a Late Spindle after Laser Cut

(A) Time lapse fluorescence images of late GFP-labeled spindles that were cut in the middle (arrow).

(B) Measurement of pole-pole distance in another cut late spindle. Scale bar = 5 μm.

still be able polymerize, suggesting that they cannot be stably capped. Thus, these behaviors predict that the spindle midzone contains factors that inhibit depolymerization at MT minus and plus ends but allow for polymerization at MT plus ends.

The extent of MT stabilization correlates with the presence of square-packed arrays of overlapping MTs in the spindle midzone, as seen in electron micrographs [10]. In early anaphase spindles, which have few packed MTs, all of the MTs depolymerize rapidly after a cut. In mid-anaphase spindles, which have extensively packed MTs through much of the spindle, the larger spindle fragments are largely stable or exhibited elongation, while very short spindle fragments connected to one SPB depolymerize. In late anaphase spindles, however, where the MTs only overlap in a short segment in the midzone, cuts cause the spindle to largely depolymerize. Thus, although molecular nature of this packing is still not clear, this packing of MTs in the spindle midzone is likely to be important to regulation of MT stability.

Force Generation in the Spindle and Role of the SPB

The continued elongation of spindles lacking one or both SPBs provides a dramatic demonstration that SPBs are not required for spindle elongation. Our results illustrate that net MT pushing forces within the spindle midzone operate during in spindle elongation. Immediately after MT cuts, the spindle fragments move abruptly inward together, suggesting that the spindle normally exerts outward-directed forces and that the nucleus (nuclear envelope, chromosomes, etc.) provides viscoelastic forces that resist movement. Astral MTs in *S. pombe* do not exert forces that pull the spindle poles apart. Indeed, fragments containing SPBs and astral MTs were not pulled to the cell tips. Rather, astral MTs may contribute pushing forces that contribute to spindle orientation during anaphase and nuclear recentering after spindle breakdown (our unpublished data). This result differs sharply from the result of laser microsurgery in the fungus *Nectria haematococca* and in PtK_2 cells, where severing of the spindle midzone accelerated pole separation during anaphase B [32–34].

Another important ramification of our results is that SPBs are dispensable for spindle elongation. What, then, is the function of SPBs? The severe chromosomal segregation defects in cut spindles show that SPBs, which attach to kinetochore MTs and chromosomes, are needed for proper chromosome segregation. In addition, SPBs may contribute to force distribution in the nuclear envelope. The spindles with only one intact SPB elongate asymmetrically, in that only the side that lacks SPB moves (until it reaches the cell tip). This behavior suggests that although the elongating spindle produces pushing forces in both directions, the resistance to movement of the SPB connected to the nuclear envelope and chromosomes is much greater than the bare nuclear envelope facing the other end of the spindle. In this view, the SPB may provide a region of structural rigidity to the nuclear envelope that facilitates nuclear movement. Another function of the SPBs is in cell cycle regulation. In mammalian cells, centrosomes are not essential for mitosis but are needed for cell cycle progression at the G_1-to-S transition [16, 35]. In *S. pombe*, components of the SIN pathway that regulate cytokinesis are localized on SPBs and are thought to be active on only one of the SPBs [27, 29]. Interestingly, we found that cutting off both SPBs, but not just one SPB, causes delays in eMTOC activation, suggesting these laser cuts may affect SIN function. However, additional studies are needed to further characterize the function of SPBs on the SIN pathway in triggering cytokinesis.

Numerous proteins have been identified that may contribute to force production and spindle stabilization in the spindle midzone. Motor proteins include Cut7p, which is a member of a homotetrameric class of kinesins (BimC and Eg5) that are able to move antiparallel MT bundles apart [11]. Ase1 is a MT bundling protein that may stabilize MT bundles; budding yeast Ase1 is required for stabilization of the spindle during anaphase B and localizes to predicted sites of MT overlap at the spindle midzone [36]. Alp14p (TOG protein) and Alp7p (TACC-like protein) may form a complex at the spindle midzone [37, 38]. Regulatory spindle midzone proteins include "chromosomal passenger" proteins, such as Aurora kinase and survivin complexes and the Clp1p/ Flp1p phosphatase [39–42]. Components of the central spindilin complex, which are important in spindle midzone function and assembly in animal cells [43], have not been identified in yeast.

Laser Ablation in Fission Yeast

These studies introduce the use of laser ablation as a new tool in yeast cell biology, which could, in principle, be used to cut or ablate many types of intracellular organelles. Laser ablation provides a high degree of spatial and temporal specificity. As shown here, this new method of physically perturbing cellular processes can provide information that cannot be obtained by using traditional approaches. The combination of laser ablation with the use of genetic tools in yeast creates a powerful synergetic approach that will undoubtedly lead to significant breakthroughs in our understanding of the mechanics and regulation of the cell division cycle.

Experimental Procedures

Yeast Strains and Preparation

S. pombe strains used in this study were: PT47 *h*$^-$ *leu1-32* pDQ105 (GFP-*atb2*), SK57 *h*$^-$ *nup107-GFP* pDQ105, FC1070 *h*$^+$ *leu1-32 ura4-d18* with integrated pREP82X-*GFP-nsp1* (*ura4*$^+$), and integrated pREP3x-SV40-GFP-lacZ (*ura4*$^+$); FC1068 *h*$^+$ *leu1-32 ura4-d18* with integrated pREP82X-*GFP-nsp1* (*ura4*$^+$) [17, 18, 24]. PT47 and SK57 were grown in the presence of thiamine, while FC1070 and FC1068 were grown in the absence of thiamine for longer than 24 hr to induce the expression of the markers. Generally, cells were grown to exponential phase in 1–2 ml shaking liquid cultures in Edinburgh minimal medium with appropriate supplements at 25°C–30°C in the dark. For slide preparation, cells were pelleted gently and placed onto 1% agarose pads containing minimal medium with supplements and were covered with a coverslip. Cells were transferred to the laser microsurgery station, where they were grown at a constant temperature of 28°C. Cells continued to undergo mitoses for at least 2–3 hr under these conditions.

Laser Microscopy/FRAP Workstation

Laser microsurgery was conducted on a custom-assembled microscopy workstation built around a Nikon TE2000E microscope (Nikon

Instruments, Inc., Melville, NY). We utilized an independent second (lower) epi-port that is available on this model to steer collimated laser beams to the back aperture of a 60×A 1.4 NA PlanApo lens. As a result, both the 532 nm beam used for laser cutting (Nd:YAG laser; 5 ns pulses, 10 Hz continuum) and the 488 nm continuous wave beam (Argon-ion laser; 15 mW) were focused on a diffraction-limited spot in the object plane. The beams were steered with custom-made dichroic mirrors (Chroma, Brattleboro, VT) that resided in the lower filter-cube turret. The top turret contained a standard "Endow" filter cube for imaging GFP fluorescence (Chroma, Brattleboro, VT). This turret was motorized so that the imaging cube could be temporarily moved out of the optical path during photobleaching routines. Because laser pulses used for microsurgery were longer in wavelength than GFP emission, it was not necessary to remove the GFP imaging cube from the optical path during laser microsurgery. This arrangement allowed us to achieve high-efficiency fluorescence while avoiding any lateral shifts in the position of the cutting beam, as are usually associated with switching between different dichroic mirrors. Further, we were able to observe the effects of laser microsurgery immediately after the cut.

All light sources in our system were shuttered by fast UniBlitz shutters (Vincent Associates, Rochester, NY) so that cells were exposed to light only during laser operations and/or image acquisition. Images were recorded with the CoolSnap HQ camera (Photometrics, Tucson, AZ). The whole system was driven by IP Lab software (Scanalytics, Fairfax, VA) run on a PC. Particular details of the lasers used in our system and the delivery path that relays the beams to the microscope are described elsewhere [44]. Some of the images were recorded as 3D datasets and are presented as maximal intensity projections.

Supplemental Data

Ten movies are available at http://www.current-biology.com/cgi/content/full/14/15/1330/DC1/.

Acknowledgments

This work was supported by National Institutes of Health grants GM 59363 (A.K.) and GM 56836 (F.C.). We thank S. Zimmerman and R. Daga for technical support, and S. Sazer for strains. Construction of laser microsurgery workstation was supported in part by a Nikon/MBL fellowship (A.K.). We thank the Marine Biological Laboratory for summer fellowships sponsored by Nikon Instruments (to A.K. and F.C.) and Universal Imaging Corporation (to F.C.) for fostering this collaboration.

Received: April 26, 2004
Revised: June 30, 2004
Accepted: July 1, 2004
Published online: July 12, 2004

References

1. Nicklas, R.B. (1997). How cells get the right chromosomes. Science *275*, 632–637.
2. Rieder, C.L., and Khodjakov, A. (2003). Mitosis through the microscope: advances in seeing inside live dividing cells. Science *300*, 91–96.
3. Rappaport, R. ed. (1996). Cytokinesis in Animal Cells (Cambridge: Cambridge University Press).
4. Khodjakov, A., Cole, R.W., and Rieder, C.L. (1997). A synergy of technologies: combining laser microsurgery with green fluorescent protein tagging. Cell Motil. Cytoskeleton *38*, 311–317.
5. Berns, M.W., Wright, W.H., and Wiegand Steubing, R. (1991). Laser microbeam as a tool in cell biology. Int. Rev. Cytol. *129*, 1–44.
6. Nabeshima, K., Nakagawa, T., Straight, A.F., Murray, A., Chikashige, Y., Yamashita, Y.M., Hiraoka, Y., and Yanagida, M. (1998). Dynamics of centromeres during metaphase-anaphase transition in fission yeast: Dis1 is implicated in force balance in metaphase bipolar spindle. Mol. Biol. Cell *9*, 3211–3225.
7. Yamamoto, A., West, R.R., McIntosh, J.R., and Hiraoka, Y. (1999). A cytoplasmic dynein heavy chain is required for oscillatory nuclear movement of meiotic prophase and efficient meiotic recombination in fission yeast. J. Cell Biol. *145*, 1233–1249.
8. Sagolla, M.J., Uzawa, S., and Cande, W.Z. (2003). Individual microtubule dynamics contribute to the function of mitotic and cytoplasmic arrays in fission yeast. J. Cell Sci. *116*, 4891–4903.
9. Hagan, I. (1998). The fission yeast microtubule cytoskeleton. J. Cell Sci. *111*, 1603–1612.
10. Ding, R., McDonald, K.L., and McIntosh, J.R. (1993). Three-dimensional reconstruction and analysis of mitotic spindles from the yeast, Schizosaccharomyces pombe. J. Cell Biol. *120*, 141–151.
11. Hagan, I., and Yanagida, M. (1990). Novel potential mitotic motor protein encoded by the fission yeast cut7+ gene. Nature *347*, 563–566.
12. Hagan, I., and Yanagida, M. (1992). Kinesin-related *cut7* protein associates with mitotic and meiotic spindles in fission yeast. Nature *356*, 74–76.
13. Berns, M.W., Aist, J., Edwards, J., Strahs, K., Girton, J., McNeill, P., Rattner, J.B., Kitzes, M., Hammer-Wilson, M., Liaw, L.H., et al. (1981). Laser microsurgery in cell and developmental biology. Science *213*, 505–513.
14. Khodjakov, A., Cole, R.W., Oakley, B.R., and Rieder, C.L. (2000). Centrosome-independent mitotic spindle formation in vertebrates. Curr. Biol. *10*, 59–67.
15. Khodjakov, A., Rieder, C.L., Sluder, G., Cassels, G., Sibon, O., and Wang, C.L. (2002). De novo formation of centrosomes in vertebrate cells arrested during S phase. J. Cell Biol. *158*, 1171–1181.
16. Khodjakov, A., and Rieder, C.L. (2001). Centrosomes enhance the fidelity of cytokinesis in vertebrates and are required for cell cycle progression. J. Cell Biol. *153*, 237–242.
17. Yoshida, M., and Sazer, S. (2004). Nucleocytoplasmic transport and nuclear envelope integrity in the fission yeast *Schizosaccharomyces pombe*. Methods *33*, 226–238.
18. Chang, F., Re, F., Sebastian, S., Sazer, S., and Luban, J. (2004). HIV-1 Vpr induces defects in mitosis, cytokinesis, nuclear structure, and centrosomes. Mol. Biol. Cell *15*, 1793–1801.
19. Khodjakov, A., Rieder, C.L., Mannella, C.A., and Kinnally, K.W. (2004). Laser micro-irradiation of mitochondria: is there an amplified mitochondrial death signal in neural cells? Mitochondrion *3*, 217–227.
20. Khodjakov, A., and Rieder, C.L. (1999). The sudden recruitment of gamma-tubulin to the centrosome at the onset of mitosis and its dynamic exchange throughout the cell cycle, do not require microtubules. J. Cell Biol. *146*, 585–596.
21. Mallavarapu, A., Sawin, K., and Mitchison, T. (1999). A switch in microtubule dynamics at the onset of anaphase B in the mitotic spindle of *Schizosaccharomyces pombe*. Curr. Biol. *9*, 1423–1426.
22. Maddox, P.S., Bloom, K.S., and Salmon, E.D. (2000). The polarity and dynamics of microtubule assembly in the budding yeast Saccharomyces cerevisiae. Nat. Cell Biol. *2*, 36–41.
23. Ding, D.Q., Chikashige, Y., Haraguchi, T., and Hiraoka, Y. (1998). Oscillatory nuclear movement in fission yeast meiotic prophase is driven by astral microtubules, as revealed by continuous observation of chromosomes and microtubules in living cells. J. Cell Sci. *111*, 701–712.
24. Tran, P.T., Marsh, L., Doye, V., Inoue, S., and Chang, F. (2001). A mechanism for nuclear positioning in fission yeast based on microtubule pushing. J. Cell Biol. *153*, 397–411.
25. Musacchio, A., and Hardwick, K.G. (2002). The spindle checkpoint: structural insights into dynamic signalling. Nat. Rev. Mol. Cell Biol. *3*, 731–741.
26. Yang, S.S., Yeh, E., Salmon, E.D., and Bloom, K. (1997). Identification of a mid-anaphase checkpoint in budding yeast. J. Cell Biol. *136*, 345–354.
27. Simanis, V. (2003). Events at the end of mitosis in the budding and fission yeasts. J. Cell Sci. *116*, 4263–4275.
28. Heitz, M.J., Petersen, J., Valovin, S., and Hagan, I.M. (2001). MTOC formation during mitotic exit in fission yeast. J. Cell Sci. *114*, 4521–4532.
29. Sohrmann, M., Schmidt, S., Hagan, I., and Simanis, V. (1998). Asymmetric segregation on spindle poles of the Schizosaccha-

romyces pombe septum-inducing protein kinase Cdc7p. Genes Dev. *12*, 84–94.
30. Maddox, P., Desai, A., Oegema, K., Mitchison, T.J., and Salmon, E.D. (2002). Poleward microtubule flux is a major component of spindle dynamics and anaphase a in mitotic *Drosophila* embryos. Curr. Biol. *12*, 1670–1674.
31. Maddox, P., Straight, A., Coughlin, P., Mitchison, T.J., and Salmon, E.D. (2003). Direct observation of microtubule dynamics at kinetochores in Xenopus extract spindles: implications for spindle mechanics. J. Cell Biol. *162*, 377–382.
32. Aist, J.R., Bayles, C.J., Tao, W., and Berns, M.W. (1991). Direct experimental evidence for the existence, structural basis and function of astral forces during anaphase B in vivo. J. Cell Sci. *100*, 279–288.
33. Aist, J.R., Liang, H., and Berns, M.W. (1993). Astral and spindle forces in PtK2 cells during anaphase B: a laser microbeam study. J. Cell Sci. *104*, 1207–1216.
34. Grill, S.W., Gonczy, P., Stelzer, E.H., and Hyman, A.A. (2001). Polarity controls forces governing asymmetric spindle positioning in the Caenorhabditis elegans embryo. Nature *409*, 630–633.
35. Hinchcliffe, E.H., Miller, F.J., Cham, M., Khodjakov, A., and Sluder, G. (2001). Requirement of a centrosomal activity for cell cycle progression through G1 into S phase. Science *291*, 1547–1550.
36. Schuyler, S.C., Liu, J.Y., and Pellman, D. (2003). The molecular function of Ase1p: evidence for a MAP-dependent midzone-specific spindle matrix. Microtubule-associated proteins. J. Cell Biol. *160*, 517–528.
37. Garcia, M.A., Vardy, L., Koonrugsa, N., and Toda, T. (2001). Fission yeast ch-TOG/XMAP215 homologue Alp14 connects mitotic spindles with the kinetochore and is a component of the Mad2-dependent spindle checkpoint. EMBO J. *20*, 3389–3401.
38. Sato, M., Vardy, L., Angel Garcia, M., Koonrugsa, N., and Toda, T. (2004). Interdependency of fission yeast Alp14/TOG and coiled coil protein Alp7 in microtubule localization and bipolar spindle formation. Mol. Biol. Cell *15*, 1609–1622.
39. Petersen, J., Paris, J., Willer, M., Philippe, M., and Hagan, I.M. (2001). The S. pombe aurora-related kinase Ark1 associates with mitotic structures in a stage dependent manner and is required for chromosome segregation. J. Cell Sci. *114*, 4371–4384.
40. Rajagopalan, S., and Balasubramanian, M.K. (2002). Schizosaccharomyces pombe Bir1p, a nuclear protein that localizes to kinetochores and the spindle midzone, is essential for chromosome condensation and spindle elongation during mitosis. Genetics *160*, 445–456.
41. Trautmann, S., Wolfe, B.A., Jorgensen, P., Tyers, M., Gould, K.L., and McCollum, D. (2001). Fission yeast Clp1p phosphatase regulates G2/M transition and coordination of cytokinesis with cell cycle progression. Curr. Biol. *11*, 931–940.
42. Cueille, N., Salimova, E., Esteban, V., Blanco, M., Moreno, S., Bueno, A., and Simanis, V. (2001). Flp1, a fission yeast orthologue of the s. cerevisiae CDC14 gene, is not required for cyclin degradation or rum1p stabilisation at the end of mitosis. J. Cell Sci. *114*, 2649–2664.
43. Mishima, M., Kaitna, S., and Glotzer, M. (2002). Central spindle assembly and cytokinesis require a kinesin-like protein/RhoGAP complex with microtubule bundling activity. Dev. Cell *2*, 41–54.
44. Cole, R.W., Khodjakov, A., Wright, W.H., and Rieder, C.L. (1995). A differential interference contrast-based light microscopic system for laser microsurgery and optical trapping of selected chromosomes during mitosis in vivo. J. Microsc. Soc. Amer. *1*, 203–215.